Analyst

Accepted Manuscript

ROYAL SOCIETY OF CHEMISTRY

www.rsc.org/analyst

Functionalized Lanthanide Coordination Polymers Nanoparticles for Selective Sensing of Hydrogen Peroxide in Biological Fluids

Hongliang Tan*, Chanjiao Ma, Qian Li, Li Wang, Fugang Xu, Shouhui Chen, Yonghai Song*

Key Laboratory of Functional Small Organic Molecule, Ministry of Education, Key Laboratory of Chemical Biology, Jiangxi Province, College of Chemistry and Chemical Engineering, Jiangxi Normal University, Nanchang, 330022, P R China

*Corresponding author: E-mail: hltan@jxnu.edu.cn (H. Tan); yhsong@jxnu.edu.cn (Y. Song)

Tel/Fax: +86 791 88120861

Table of contents entry

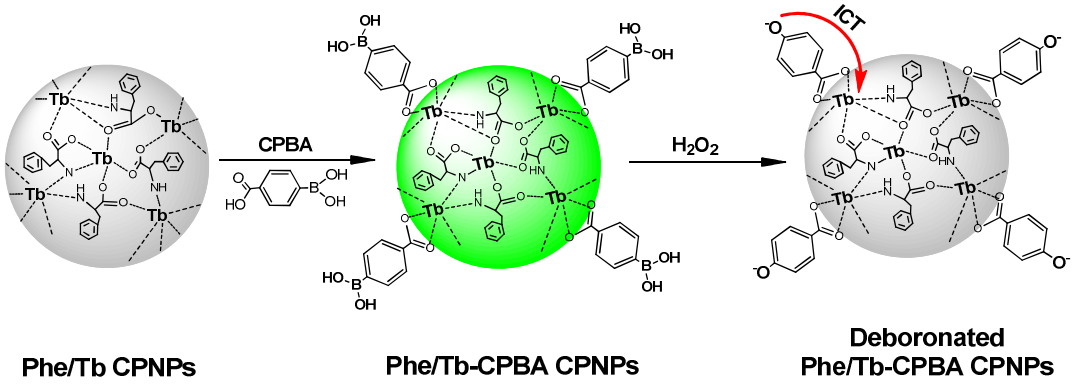

The fluorescence of Phe/Tb CPNPs functionalized with CPBA (Phe/Tb-CPBA CPNPs) was selectively quenched upon the addition of H_2O_2.

Abstract

Lanthanide coordination polymers have been emerged as very fascinating sensing materials due to their tunable structures and unique optical properties. However, a major problem concerning the applications of lanthanide coordination polymers for fluorescent sensing is their unselective recognition to analytes. In this work, a direct post-modification strategy was employed to prepare a functionalized lanthanide coordination polymer nanoparticles (Phe/Tb-CPBA CPNPs) with specific response ability to hydrogen peroxide (H_2O_2) by using phenylalanine (Phe) as bridging ligands, terbium ions (Tb^{3+}) as metal nodes and carboxyphenylboronic acid (CPBA) as guest ligands. The Phe/Tb-CPBA CPNPs emits a strong green fluorescence due to the removal of coordinated water molecules and the sensitization effect of CPBA. Upon the addition of H_2O_2, however, quenched fluorescence of Phe/Tb-CPBA CPNPs can be observed owing to an intramolecular charge transfer effect. This finding led to a method for the quantitation of H_2O_2 in the 6 μM to 1 mM concentration range and with a detection limit at 2 μM. Because of the chemoselective of H_2O_2-mediated oxidative deboronation, the Phe/Tb-CPBA CPNPs as a fluorescent sensor exhibits excellent selectivity to H_2O_2. Furthermore, the Phe/Tb-CPBA CPNPs was successfully used to measure the level of H_2O_2 in urine samples and showed satisfactory results. We envision that the presented strategy could be extended to design other functionalized coordination polymers with desire functions for various biomedical applications.

Keywords: Lanthanide coordination polymers nanoparticles, Functionalization, Fluorescent sensing, Hydrogen peroxide

Introduction

Coordination polymers constructed from metal ions and organic bridging ligands have recently emerged as very interesting functional materials due to their tunable structures and properties. A diverse choice of building blocks affords an infinite number of coordination polymers with different architectures and physicochemical properties, and hence the applications of coordination polymers in many different areas could be founded. To date, coordination polymers have already been used in many fields, such as gas storage and separation, [1] liquid chromatography separation, [2] heterogeneous catalysis, [3] drug delivery, [4, 5] biomedical imaging, [6] and chemical sensing. [7] In particular, the explorations of coordination polymers as fluorescent sensing materials have attracted considerable attentions.[8] Compared with conventional sensing materials, coordination polymers possess the advantages of structural and chemical diversity, excellent thermal stability and processability, and intrinsic biodegradability.[9] Among the coordination polymers used for fabricating fluorescent sensors, lanthanide coordination polymers are particularly interested due to their unique optical properties, such as large Storks shift, high quantum yields, and long lifetime. Currently, some lanthanide coordination polymers have been used as fluorescent probes for the detection of metal ions, [10-12] anions [13, 14] and small molecules. [15, 16] However, most of the detection reactions were performed in organic media and in solid state owing to their macroscopic size and the use of synthetic organic molecules as bridging ligands. This hinders their further applications as fluorescent probes in biomedical field. Natural biomolecules are attractive bridging ligands for the construction of metal-organic coordination polymers due to their inherent properties, such as diverse chemical structures, multiple metal-binding sites, low toxicity, and good biocompatibility.[17] So, the incorporation of biomolecules usually can afford the coordination polymers to some new or enhanced properties that cannot be accessed by using organic molecules as bridging ligands.

Recently, some nanoscaled lanthanide coordination polymers with good environmental compatibility and attractive fluorescent behaviors have been prepared by using water-soluble nucleotide or nucleobase as bridge ligands. [18-20] Due to the quenching effect of water molecules, these lanthanide coordination polymers themselves displayed very weak fluorescence. Upon the

chelation of lanthanide ions by suitable aromatic ligands that can transfer energy to the emissive state of lanthanide ions, however, the weak fluorescence of these lanthanide coordination polymers can be enhanced significantly. Based on this mechanism, several lanthanide receptor platforms for direct detecting small molecules in aqueous solution have been developed. [21, 22] In spite of this, the rational design and potential applications of lanthanide coordination polymers-based fluorescent sensors are still in an initial stage. Particularly, the improvement in the selectivity of lanthanide coordination polymers to analytes in complicated environment remains great challenges because that the unspecific binding of other aromatic ligands to lanthanide ions may give rise to false positives. [23] For conventional inorganic nanomaterials-based sensors, an often-used way to obtain high selectivity is the surface functionalization of nanomateials with suitable guest ligands that can specific response to analytes. [24, 25] Nevertheless, the examples of using post-modification strategy to construct coordination polymers-based selective fluorescent sensors are very few, especially the sensors based on lanthanide coordination polymers. Very recently, based on post-modification strategy, Chen group [26] and Lv group [27, 28] prepared several fluorescent coordination polymers composites by encapsulating fluorescent nanomaterials including carbon dots, graphene oxide and ZnO quantum dots, respectively. They demonstrated that these coordination polymers composites have better water dispersibility than their parent counterparts and can be used to detection of metal ions and anion due to the selective recognition of the encapsulated nanomaterials to analytes. These studies are attractive for the sensing applications of coordination polymers, but they are limited by the macroscopic sizes of parent coordination polymers and/or the time-consumed preparation procedures of the guest nonamaterials.

Hydrogen peroxide (H_2O_2) is an important chemical which has been widely used for paper bleaching, medical and pharmaceutical sterilization, and waste water treatment. In living organisms, on the other hand, H_2O_2 is a component of cell signaling pathways that are necessary for the growth, development, and fitness of living organisms.[29] Also, H_2O_2 is one of major reactive oxygen species in living organisms. The overproduction and/or mismanagement of H_2O_2 can lead to the general phenomenon of oxidative stress that is implicated with various diseases including diabetes, cancer, cardiovascular and neurodegenerative disorders.[30] Particularly, the level of H_2O_2

in urine has recently been suggested as a potential biomarker of whole body oxidative stress.[31] Therefore, the accurate and selective detection of H_2O_2 is of great importance in clinical chemistry, analytical biochemistry and environmental science. Up to now, many methods have been developed for the detection of H_2O_2, such as spectrophotometry,[32] spectrofluorimetry,[33] electrochemistry,[34] and colorimetric analysis [35]. Among these methods, fluorescent detection for H_2O_2 would be a more desirable method because of its operational simplicity and high sensitivity, especially lanthanide ions-based fluorescent detection.[36-39] The long wavelength emission and long fluorescent lifetimes of lanthanide ions allow the detection of H_2O_2 *via* time-delay mode, which can eliminate efficiently the interferences from background and scattering fluorescence. Nevertheless, most of the lanthanide fluorescent probes for H_2O_2 detection have been limited to molecular lanthanide compounds.

In this work, we attempt to employ a direct post-modification strategy to fabricate a kind of functionalized lanthanide coordination polymer nanoparticles (CPNPs) and utilize the CPNPs as a fluorescent probe for selective detection of H_2O_2. The construction of functionalized lanthanide coordination polymer nanoparticles (Phe/Tb-CPBA CPNPs) is based on the chemical coordination of 4-carboxyphenylboronic acid (CPBA) with their parent CPNPs (Phe/Tb CPNPs) prepared from phenylalanine (Phe, acting as bridge ligands) and terbium ions (Tb^{3+}, action as metal nodes). As an attractive bridging ligand, Phe with flexible structure can coordinate with Tb^{3+} through its carboxyl and amino groups to built Phe/Tb CPNPs. [40] The Phe/Tb CPNPs displayed very weak fluorescence due to the quenching effect of coordinated water molecules. Upon the complexation of CPBA with Phe/Tb CPNPs, however, enhanced fluorescence of Tb^{3+} can be observed because of the removal of coordinated water molecules and the sensitization effect of CPBA.[36, 41] Owing to the chemoseletivity of H_2O_2-induced deboronation, on the other hand, the addition of H_2O_2 could hydrolyze the boronic acid group of CPBA, and leading to the formation of 4-oxo anion at CPBA residue. When excited with light, an intramolecular charge transfer (ICT) process from the formed 4-oxo anion to emissive state of lanthanide ions may be occurred, which can result in the quenching of the fluorescence of lanthanide ions.[37] Therefore, quenched fluorescence of Phe/Tb-CPBA CPNPs in the presence of H_2O_2 is expected to be observed (**Scheme 1**).

Scheme 1

Experimental section

Chemicals

All chemical are obtained from commercial source and used without further purification. Terbium nitrate ($Tb(NO_3)_3 \cdot 6H_2O$, 99.99%) was purchased from Rewin Rare Earth Metal Materials Co., Ltd (Baotou, China); 4-carboxyphenylboronic acid (CPBA), phenylalanine (Phe), aspartic acid (Asp), glutamic acid (Glu), and tryptophan (Try) were obtained from Aladdin (Shanghai, China); Metal salts (NaCl, KCl, $MgCl_2$, $CaCl_2$, Na_2SO_4), uric acid (UA), urea and creatinine (Cr)were purchased from Sinopharm Chemical Reagent Co. Ltd (Shanghai, China). Ultrapure water (18 MΩ cm) was used for the preparation of all aqueous solutions. Unless otherwise stated, all chemicals are of analytical reagent grade.

Instruments

The morphology of coordination polymers was measured by S-3400 scanning electron microscopy (SEM, Hitachi, Japan) equipped with an energy dispersive spectra (EDS) detector. Fluorescence spectra were recorded on F-7000 fluorescence spectrophotometer (Hitachi, Japan). A 240 nm excitation wavelength was used to record the emission spectra, whereas the excitation spectra were recorded by setting the emission intensity at 545 nm. The UV-visible absorption spectra were measured by using Lambda35 spectrophotometer (PerkinElmer, UK). Avatar 360 FTIR spectrometer (Nicolet, USA) was used to record the Fourier transform infrared (FTIR) spectra with the KBr pellet technique. The analysis of X-ray photoelectron spectra (XPS) and powder X-Ray diffraction (XRD) spectrum were performed on Axis Ultra DLD X-ray Photoelectron Spectroscope (Hitachi, Japan) and D8 Advance X-Ray diffractometer (Bruker, Germany), respectively.

Preparation of Phe/Tb CPNPs

A solvothermal method was employed to prepare the coordination polymers Phe/Tb. Typically, 2 mL of $Tb(NO_3)_3$ aqueous solution (40 mM) was added dropwise to the mixture containing 5 mL of

Phe aqueous solution (40 mM) and 5 mL of N,N-dimethylformamide (DMF) under stirring. After incubating for 20 min at room temperature (25 ℃, the same as below), the mixture was placed in 50 mL Teflon-lined stainless steel autoclave and heated to at 150 °C for reacting 4 h. The products were collected by centrifugation (13000 rpm, 10 min) after cooling to room temperature. To remove unreacted reactants, the precipitations were washed with absolute ethanol for several times. Then, the Phe/Tb CPNPs was dispersed in absolute ethanol for further use.

Preparation of Phe/Tb-CPBA CPNPs

The Phe/Tb-CPBA CPNPs was obtained by chemical coordination of CPBA with parent CPBA. Briefly, excess amounts of CPBA (10 mM) were added dropwise to 1 mL of parent Phe/Tb suspension under stirring. After reacting for 12 h at room temperature, the products were collected by centrifugation. The precipitates were washed several times with absolute ethanol to remove unbounded CPBA. The obtained solid materials were dispersed in 1 mL of ethanol to obtain Phe/Tb-CPBA CPNPs suspension. The amounts of CPBA on the surface of Phe/Tb were determined by measuring the UV-visible absorption of CPBA at 235 nm.

Detection of H_2O_2 in aqueous solution

The experiment of fluorescent response of Phe/Tb-CPBA CPNPs to H_2O_2 was performed at room temperature. Briefly, various amounts of H_2O_2 with final concentrations from 0 to 10 mM were added to the mixture of 5 μL Phe/Tb-CPBA CPNPs suspension and HEPES buffer at pH 7.0, respectively, and the reaction solutions were incubated for 20 min at room temperature. The final volume of these reaction solutions are 200 μL. The fluorescent spectra of these reaction solutions were then recorded with a 240 nm excitation wavelength and the decreased fluorescent intensity of these reaction solutions at 545 nm was used for the quantitative analysis of H_2O_2. To examine the effect of interferential substances on the fluorescent assay of Phe/Tb-CPBA CPNPs for H_2O_2, 10 μL of 10mM amino acids (Glu, Asp, Try), metal salts (NaCl, KCl, $MgCl_2$, $CaCl_2$, Na_2SO_4), UA urea and Cr were added to Phe/Tb-CPBA CPNPs solution, respectively. The total volume was reached to 200 μL by adding HEPES buffer. After reacting for 20 min, the fluorescent spectra of the reaction solutions were measured.

Determination of H_2O_2 in urine samples

Urine samples were collected from healthy adult volunteer and diluted for 10 folds for pretreatment. To prepare spiked urine samples, different amounts of H_2O_2 were added to the diluted urine samples. The final concentrations of added H_2O_2 in spiked urine samples are in the range of 0 to 1 mM. The Phe/Tb-CPBA CPNPs suspension (5 μL) was added to the spiked urine samples. The reaction solutions were incubated for 20 min before measuring their fluorescence spectra.

Results and discussion

To obtain functionalized Phe/Tb CPNPs, its parent counterpart Phe/Tb CPNPs was firstly synthesized by a solvothermal reaction. The morphology of the as-prepared Phe/Tb CPNPs was examined by scanning electron microscopy (SEM). As shown in **Fig. 1a**, Phe/Tb CPNPs are spherical with average size of 670 nm. The powder XRD data of Phe/Tb CPNPs indicate that they are structurally amorphous (**Fig. S1a**). The chemical compositions of Phe/Tb CPNPs were determined by energy-dispersed spectrum (EDS) and X-ray photoelectron spectrum (XPS). The peaks of Tb, C, N and O elements can be founded from the EDS and XPS spectrum of Phe/Tb CPNPs (**Fig. 1c** and **1d**), indicating that Phe and Tb^{3+} were involved in the construction of Phe/Tb CPNPs. Compared with pure Phe, the changes of Phe/Tb CPNPs in the FTIR spectra of carboxyl (from 1596 to 1577 cm^{-1}) and amino group (from 1494 to 1519 cm^{-1}) reflect the occurrence of the coordination interactions between Phe and Tb^{3+} (**Fig. S2**). [42] With the coordination of CPBA with unsaturated Tb^{3+} on the surface of Phe/Tb CPNPs, functionalized Phe/Tb CPNPs (Phe/Tb-CPBA CPNPs) was achieved. From **Fig. 1b**, it can be seen that Phe/Tb-CPBA CPNPs displayed almost no changes in the shape and size compared with parent Phe/Tb CPNPs. Like parent Phe/Tb CPNPs, the Phe/Tb-CPBA CPNPs are also amorphous (**Fig. S1b**). The results imply that the loading of CPBA has no influence on the morphology and structure of its parent Phe/Tb CPNPs.

Figure 1

To verify the coordination of CPBA with Phe/Tb CPNPs, the Phe/Tb-CPBA CPNPs was

characterized by FTIR and XPS. Compared with the FTIR spectrum of parent Phe/Tb CPNPs alone, two new peaks at 1385 and 1410 cm^{-1} were observed from Phe/Tb-CPBA CPNPs (**Fig. 2A**). These two peaks can be assigned to B-O and C-B stretching vibrations of CPBA, respectively,[43, 44] which implies the presence of CPBA on the surface of Phe/Tb CPNPs. In addition, the XPS peaks correspond to C-B bond at 189.6 eV in the O1s spectrum [45] and B-O bond and at 533.3 eV in the B1s spectrum [46] were founded in Phe/Tb-CPBA CPNPs (**Fig.S3**). The appearance of C-B and B-O bond in the XPS spectra of Phe/Tb-CPBA CPNPs further indicates that the CPBA was immobilized on the surface of Phe/Tb CPNPs. By comparison with pure CPBA, furthermore, an obvious shift at C=O stretching vibrations of the carboxyl group of CPBA in Phe/Tb-CPBA CPNPs from 1686 to 1595 cm^{-1} was observed. This reflects that CPBA was not adsorbed on the surface of Phe/Tb CPNPs but involved in the coordination of Tb^{3+} through its carboxyl group, which leads to the formation of Phe/Tb-CPBA CPNPs. It is well known that the coordination of aromatic ligands allowed π-π^* transition with lanthanide ions usually leads to the changes of their absorption peaks. [19] So, the absorption spectra of free CPBA, Phe/Tb CPNPs and Phe/Tb-CPBA CPNPs were investigated. As shown in **Fig. 2B**, free CPBA displayed a maximum absorption peak at 235 nm, whereas an absorption peak at 231 nm was observed from Phe/Tb-CPBA CPNPs. The peak of Phe/Tb-CPBA CPNPs at 231 nm is resulted from the blue shift of free CPBA after coordinating with Phe/Tb CPNPs. The changed absorption spectra further confirm that the coordination interaction between CPBA and Tb^{3+} on the surface of Phe/Tb CPNPs was occurred.

Figure 2

Then, we studied the fluorescent properties of Phe/Tb-CPBA CPNPs. As shown in **Fig. 3**, Phe/Tb CPNPs exhibited very weak fluorescence, which may result from the O-H vibration of coordinated water molecules. However, a strong fluorescence with emission peaks at 485, 545, 585, and 620 nm can be observed from Phe/Tb-CPBA CPNPs. These four peaks are typical emissions of Tb^{3+} and correspond to the $^5D_4$ to ^7F_j (j = 3-6) electronic transitions of Tb^{3+}, respectively. [47] The result reflects that the CPBA not only coordinates with Tb^{3+} on the surface of Phe/Tb CPNPs, but also sensitize the fluorescence of Tb^{3+}. The fluorescence quantum yields of Phe/Tb-CPBA CPNPs were determined relative to quinine sulfate (ϕ = 0.54) in 1 M sulfuric acid, [48] and which was

founded to be 0.03 in water. In the presence of H_2O_2, however, the fluorescence of the Phe/Tb-CPBA was decreased drastically. The decreased fluorescence of Phe/Tb-CPBA may be attributed to the ICT effect of 4-oxo anion produced by H_2O_2-induced oxidative deboronation of CPBA. [37] Nevertheless, the excitation spectra of Phe/Tb-CPBA CPNPs displayed no changes upon the addition of H_2O_2. This result suggests that the added H_2O_2 have no influence on the inherent transition processes of Tb^{3+} induced by the ligand-field.

Figure 3

In order to understand the interaction between Phe/Tb-CPBA CPNPs and H_2O_2, the FTIR spectra of Phe/Tb-CPBA CPNPs in the absence and presence of H_2O_2 were analyzed. As shown in **Fig. S4**, after reacting with H_2O_2, the B-O stretching vibrations at 1385 and 1410 cm^{-1} and the B-C stretching vibrations at 1481 cm^{-1} of Phe/Tb-CPBA CPNPs were disappeared. The aryl group of CPBA on the surface of Phe/Tb-CPBA CPNPs treated with H_2O_2 at 1083 cm^{-1} displayed much broader than their counterparts. [49] The FTIR spectra changes of Phe/Tb-CPBA CPNPs in the presence of H_2O_2 indicate the hydrolysis of boronic acid group of CPBA on the surface of Phe/Tb CPNPs, which was confirmed by the disappearance of the B-O band at 533.3 eV in the B (1s) spectrum of Phe/Tb-CPBA CPNPs treated with H_2O_2 (**Fig. S3b**). In addition, the absorption spectra of Phe/Tb-CPBA CPNPs in the presence of H_2O_2 with different concentrations were measured. After the addition of H_2O_2, almost no changes were observed in the absorption spectra of Phe/Tb-CPBA CPNPs (**Fig. S5**); even the H_2O_2 concentration was increased to 1 mM. The results indicate that the added H_2O_2 only hydrolyze the boronic acid group of CPBA and does not affect the chemical structure of benzene ring of CPBA, and that the chemical coordination between Phe/Tb CPNPs and CPBA remained unchanged in the presence of H_2O_2. Furthermore, there are no changes in the shape and size of Phe/Tb-CPBA CPNPs after reacting with H_2O_2 (**Fig. S6**).

Figure 4

To evaluate the feasibility of Phe/Tb-CPBA CPNPs as a fluorescent probe for H_2O_2, we

investigated its fluorescent response to H_2O_2 at different experimental conditions. As shown in **Fig. S7**, Phe/Tb-CPBA CPNPs exhibited a fast fluorescent response rate to H_2O_2. The fluorescence of Phe/Tb-CPBA CPNPs can be quenched completely within 20 min. The pH of reaction media showed serious affects on the fluorescence of Phe/Tb-CPBA CPNPs. From **Fig. S8**, it can be seen that Phe/Tb-CPBA CPNPs has a maximum fluorescent intensity at neutral media with pH 7.0. In strong acid or base media, however, the fluorescence of Phe/Tb-CPBA CPNPs was quenched significantly. The results may be ascribed to the protonation of Phe and CPBA in strong acid media and the formation of terbium hydroxide precipitation in strong base media, which results in the dissociation of Phe/Tb-CPBA CPNPs. Under the optimized conditions, the fluorescent intensities of Phe/Tb-CPBA CPNPs in the presence of H_2O_2 with different concentrations were measured. As shown in **Fig. 4**, the fluorescent intensity of Phe/Tb-CPBA CPNPs decreased gradually with the increase of H_2O_2 concentrations. There is a linear relationship between the fluorescent intensity of Phe/Tb-CPBA CPNPs at 545 nm and H_2O_2 concentrations in the range of 6 μM to 2 mM. The detection limit for H_2O_2 is 2 μM on the basis of a signal-to-noise ratio of 3:1. In addition, we compared the presented method with some existed methods for the detection of H_2O_2 (**Table S1**). Compared with the previously reported methods, our method not only showed a very comparable detection limit, but also the preparation of Phe/Tb-CPBA CPNPs is easier, which does not involve in laborious chemical synthesis, and the present detection procedure has a lower cost. Moreover, Phe/Tb-CPBA CPNPs possesses a long enough emission lifetime for time-resolved fluorescent assays. Taking into account the advantages, Phe/Tb-CPBA CPNPs as a fluorescent probe holds great potential for the detection of H_2O_2 in biological samples.

Figure 5

The specific response of Phe/Tb-CPBA CPNPs to H_2O_2 was examined by measuring the fluorescent intensity of Phe/Tb-CPBA CPNPs in the solutions containing the substances coexisted in biological fluids. It is well known that some common inorganic cations and anions, uric acid (UA), urea, creatinine (Cr) and amino acids are presented in human urine, which may affect the fluorescence of Phe/Tb-CPBA CPNPs by either reacting with CPBA or coordinating with Tb^{3+}. So, the substances including Na^+, K^+, Mg^{2+}, Ca^{2+}, SO_4^{2-}, Cl^-, UA, urea, Cr, Glu, Asp, and Try were

selected as representative interferences to study the selectivity of Phe/Tb-CPBA CPNPs to H_2O_2. As shown in **Fig. 5**, only H_2O_2 caused a significant decrease in the fluorescence of Phe/Tb-CPBA CPNPs, whereas the presence of these interferences showed negligible influences on the fluorescence of Phe/Tb-CPBA CPNPs. Even the concentrations of these interferences were increased to 10 mM; the fluorescence of Phe/Tb-CPBA CPNPs is still no obvious changes. The excellent selectivity of Phe/Tb-CPBA CPNPs can be attributed to the chemical selectivity of H_2O_2-induced oxidative deboronation of aryl boronic acids. [36] Therefore, Phe/Tb-CPBA CPNPs appears to be useful for selectively sensing H_2O_2 in biological fluids.

The performance of Phe/Tb-CPBA CPNPs as a fluorescent sensor for H_2O_2 detection was tested by using the human urine as real sample. The urine sample was collected from healthy volunteer and diluted 10 fold for pretreatment. The standard addition method was used for the detection of H_2O_2 in urine samples. The results were displayed in **Table S2**. It was found that the recoveries of H_2O_2 in urine samples are more than 98% and the relative standard deviations are less than 7.70%. The results indicate that the level of H_2O_2 in urine sample can be accurately detected with good recovery and precision by using Phe/Tb-CPBA CPNPs as a fluorescent sensor.

Conclusions

In summary, a kind of functionalized lanthanide coordination polymer nanoparticles (Phe/Tb-CPBA CPNPs) with selective fluorescent sensing function has been constructed by employing a direct post-modification strategy. The Phe/Tb-CPBA CPNPs emits a strong fluorescence of Tb^{3+} due to the removal of water molecules from Tb^{3+} coordination sphere and the sensitization effect of CPBA. In the presence of H_2O_2, however, obviously quenched fluorescence can be observed from the Phe/Tb-CPBA CPNPs because of the ICT effect of 4-oxy anion formed by the oxidative deboronation of CPBA. The fluorescent intensity of Phe/Tb-CPBA CPNPs decreased linearly with the increase of H_2O_2 concentration from 6 μM to 1 mM, and a detection limit of 2 μM was obtained. As a fluorescent sensor, Phe/Tb-CPBA CPNPs exhibited excellent selectivity to H_2O_2 due to the chemoselective of H_2O_2-mediated oxidative deboronation. To the best of our knowledge, this is the first report about the construction and application of selective fluorescent sensor based on functionalized lanthanide coordination polymers. The practical

application of Phe/Tb-CPBA CPNPs as a fluorescent probe was exploited by the measurement of the level of H_2O_2 in urine sample and satisfactory results can be obtained. We believe that the presented strategy might create new avenues for the construction of functionalized coordination polymers with desire functions and subsequently a wider application of lanthanide coordination polymers is expected.

Acknowledgements

This work was supported by the Natural Science Foundation of China (No. 21305054), Start-up Funding of Jiangxi Normal University, Specialized Research Fund for the Doctoral Program of Higher Education of China (No. 20133604120002), Scientific Research Foundation of Education Commission of Jiangxi Province (No. GJJ14258).

References

1. J.-R. Li, R. J. Kuppler and H.-C. Zhou, *Chem. Soc. Rev.*, 2009, **38**, 1477-1504.
2. C.-X. Yang, Y.-J. Chen, H.-F. Wang and X.-P. Yan, *Chem. Eur. J.*, 2011, **17**, 11734-11737.
3. J. Lee, O. K. Farha, J. Roberts, K. A. Scheidt, S. T. Nguyen and J. T. Hupp, *Chem. Soc. Rev.*, 2009, **38**, 1450-1459.
4. P. Horcajada, T. Chalati, C. Serre, B. Gillet, C. Sebrie, T. Baati, J. F. Eubank, D. Heurtaux, P. Clayette, C. Kreuz, J.-S. Chang, Y. K. Hwang, V. Marsaud, P.-N. Bories, L. Cynober, S. Gil, G. Ferey, P. Couvreur and R. Gref, *Nat Mater*, 2010, **9**, 172-178.
5. P. F. Gao, L. L. Zheng, L. J. Liang, X. X. Yang, Y. F. Li and C. Z. Huang, *J. Mater. Chem. B*, 2013, **1**, 3202-3208.
6. F. Novio, J. Simmchen, N. Vázquez-Mera, L. Amorín-Ferré and D. Ruiz-Molina, *Coord. Chem. Rev.*, 2013, **257**, 2839-2847.
7. L. E. Kreno, K. Leong, O. K. Farha, M. Allendorf, R. P. Van Duyne and J. T. Hupp, *Chem. Rev.*, 2012, **112**, 1105-1125.
8. Y. Cui, Y. Yue, G. Qian and B. Chen, *Chem. Rev.*, 2012, **112**, 1126-1162.
9. J. Della Rocca, D. Liu and W. Lin, *Acc. Chem. Res.*, 2011, **44**, 957-968.
10. W. Yang, J. Feng and H. Zhang, *J. Mater. Chem.*, 2012, **22**, 6819-6823.
11. Z. Hao, X. Song, M. Zhu, X. Meng, S. Zhao, S. Su, W. Yang, S. Song and H. Zhang, *J. Mater.*

Chem. A, 2013, **1**, 11043-11050.

12. C.-X. Yang, H.-B. Ren and X.-P. Yan, *Anal. Chem.*, 2013, **85**, 7441-7446.
13. K. L. Wong, G. L. Law, Y. Y. Yang and W. T. Wong, *Adv. Mater.*, 2006, **18**, 1051-1054.
14. B. Chen, L. Wang, F. Zapata, G. Qian and E. B. Lobkovsky, *J. Am. Chem. Soc.*, 2008, **130**, 6718-6719.
15. Y. Qiu, H. Deng, J. Mou, S. Yang, M. Zeller, S. R. Batten, H. Wu and J. Li, *Chem. Commun.*, 2009, 5415-5417.
16. B. Gole, A. K. Bar and P. S. Mukherjee, *Chem. Commun.*, 2011, **47**, 12137-12139.
17. I. Imaz, M. Rubio-Martinez, J. An, I. Sole-Font, N. L. Rosi and D. Maspoch, *Chem. Commun.*, 2011, **47**, 7287-7302.
18. H. Tan, B. Liu and Y. Chen, *ACS Nano*, 2012, **6**, 10505-10511.
19. C. Aimé, R. Nishiyabu, R. Gondo and N. Kimizuka, *Chem. Eur. J.*, 2010, **16**, 3604-3607.
20. R. Nishiyabu, N. Hashimoto, T. Cho, K. Watanabe, T. Yasunaga, A. Endo, K. Kaneko, T. Niidome, M. Murata, C. Adachi, Y. Katayama, M. Hashizume and N. Kimizuka, *J. Am. Chem. Soc.*, 2009, **131**, 2151-2158.
21. H. Tan, C. Ma, Y. Song, F. Xu, S. Chen and L. Wang, *Biosens. Bioelectron.*, 2013, **50**, 447-452.
22. H. Tan, L. Zhang, C. Ma, Y. Song, F. Xu, S. Chen and L. Wang, *ACS Appl. Mater. Interfaces*, 2013, **5**, 11791-11796.
23. M. L. Cable, J. P. Kirby, K. Sorasaenee, H. B. Gray and A. Ponce, *J. Am. Chem. Soc.*, 2007, **129**, 1474-1475.
24. S. G. Penn, L. He and M. J. Natan, *Curr. Opin. Chem. Biol.*, 2003, **7**, 609-615.
25. J. Liu, X. Yang, X. He, K. Wang, Q. Wang, Q. Guo, H. Shi, J. Huang and X. Huo, *Sci. China Chem.*, 2011, **54**, 1157-1176.
26. X. Lin, G. Gao, L. Zheng, Y. Chi and G. Chen, *Anal. Chem.*, 2014, **86**, 1223-1228.
27. L. Hao, H. Song, Y. Su and Y. Lv, *Analyst*, 2014, **139**, 764-770.
28. D. Zhao, X. Wan, H. Song, L. Hao, Y. Su and Y. Lv, *Sens. Actuators B-Chem.*, 2014, **197**, 50-57.
29. D. Liu, K. Lu, C. Poon and W. Lin, *Inorg. Chem.*, 2014, **53**, 1916-1924.
30. G. C. Van de Bittner, E. A. Dubikovskaya, C. R. Bertozzi and C. J. Chang, *Proc. Natl. Acad. Sci.*, 2010, **107**, 21316-21321.

31. J. W. M. Yuen and I. F. F. Benzie, *Free Radical Res.*, 2003, **37**, 1209-1213.

32. K. Sunil and B. Narayana, *Bull. Environ. Contam. Toxicol.*, 2008, **81**, 422-426.

33. D. Srikun, E. W. Miller, D. W. Domaille and C. J. Chang, *J. Am. Chem. Soc.*, 2008, **130**, 4596-4597.

34. J. Bai and X. Jiang, *Anal. Chem.*, 2013, **85**, 8095-8101.

35. L. Hu, Y. Yuan, L. Zhang, J. Zhao, S. Majeed and G. Xu, *Anal. Chim. Acta*, 2013, **762**, 83-86.

36. A. R. Lippert, T. Gschneidtner and C. J. Chang, *Chem. Commun.*, 2010, **46**, 7510-7512.

37. M. Liu, Z. Ye, G. Wang and J. Yuan, *Talanta*, 2012, **91**, 116-121.

38. O. S. Wolfbeis, A. Dürkop, M. Wu and Z. Lin, *Angew. Chem. Int. Ed.*, 2002, **41**, 4495-4498.

39. C. Lv, W. Di, Z. Liu, K. Zheng and W. Qin, *Analyst*, 2014, DOI: 10.1039/C4AN00952E.

40. Y. Liu and Z. Tang, *Chem. Eur. J.*, 2012, **18**, 1030-1037.

41. A. R. Lippert, G. C. Van de Bittner and C. J. Chang, *Acc. Chem. Res.*, 2011, **44**, 793-804.

42. R. Mahalakshmi, S. X. Jesuraja and S. J. Das, *Cryst. Res. Technol.*, 2006, **41**, 780-783.

43. W.-K. Oh, Y. S. Jeong, S. Kim and J. Jang, *ACS Nano*, 2012, **6**, 8516-8524.

44. P. Shen and Y. Xia, *Anal. Chem.*, 2014.

45. D. Das, D.-M. Kim, D.-S. Park and Y.-B. Shim, *Electroanal.*, 2011, **23**, 2036-2041.

46. S. Y. Song and H. C. Yoon, *Sens. Actuators B-Chem.*, 2009, **140**, 233-239.

47. F. S. Richardson, *Chem. Rev.*, 1982, **82**, 541-552.

48. S. Petoud, S. M. Cohen, J.-C. G. Bünzli and K. N. Raymond, *J. Am. Chem. Soc.*, 2003, **125**, 13324-13325.

49. R. Mahalakshmi, J. M. Linet, S. N. Priya, B. M. Boaz, S. X. Jesuraja and S. J. Das, *Cryst. Res. Technol.*, 2006, **41**, 1072-1075.

Figure captions

Scheme 1. Illumination of fluorescent response of Phe/Tb-CPBA CPNPs to H_2O_2.

Figure 1. SEM images of Phe/Tb CPNPs (a) and Phe/Tb-CPBA CPNPs (b) and the EDS spectrum (c) and XPS spectrum (d) of Phe/Tb CPNPs.

Figure 2. A is the FTIR spectra of pure CPBA (a) and Phe/Tb-CPBA CPNPs (b) and B is the absorption spectra of Phe/Tb CPNPs (a), CPBA (b) and Phe/Tb-CPBA CPNPs (c).

Figure 3. Excitation and emission spectra of Phe/Tb CPNPs (a), Phe/Tb-CPBA CPNPs (b), and Phe/Tb-CPBA CPNPs in the presence of 800 μM H_2O_2 (c).

Figure 4. Fluorescent spectra of Phe/Tb-CPBA CPNPs in the presence H_2O_2 with different concentrations (a) and linear relationship of the fluorescent intensity of Phe/Tb-CPBA CPNPs at 545 nm with respect to H_2O_2 concentrations (b).

Figure 5. Effects of interferences (each 1 mM) on the fluorescent intensity of Phe/Tb-CPBA CPNPs at 545 nm.

Schemes and figures

Scheme 1

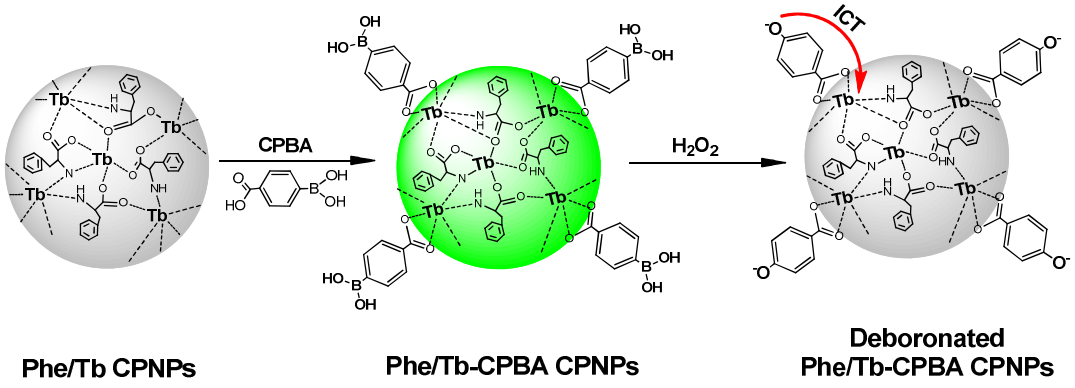

Figure 1

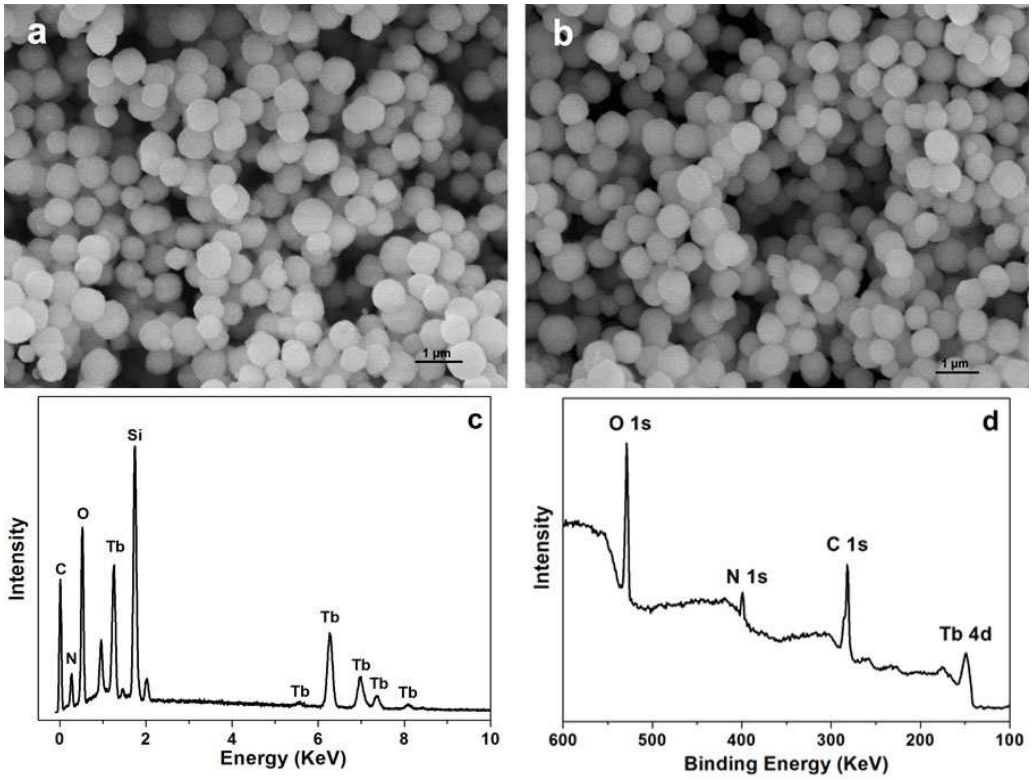

Figure 2

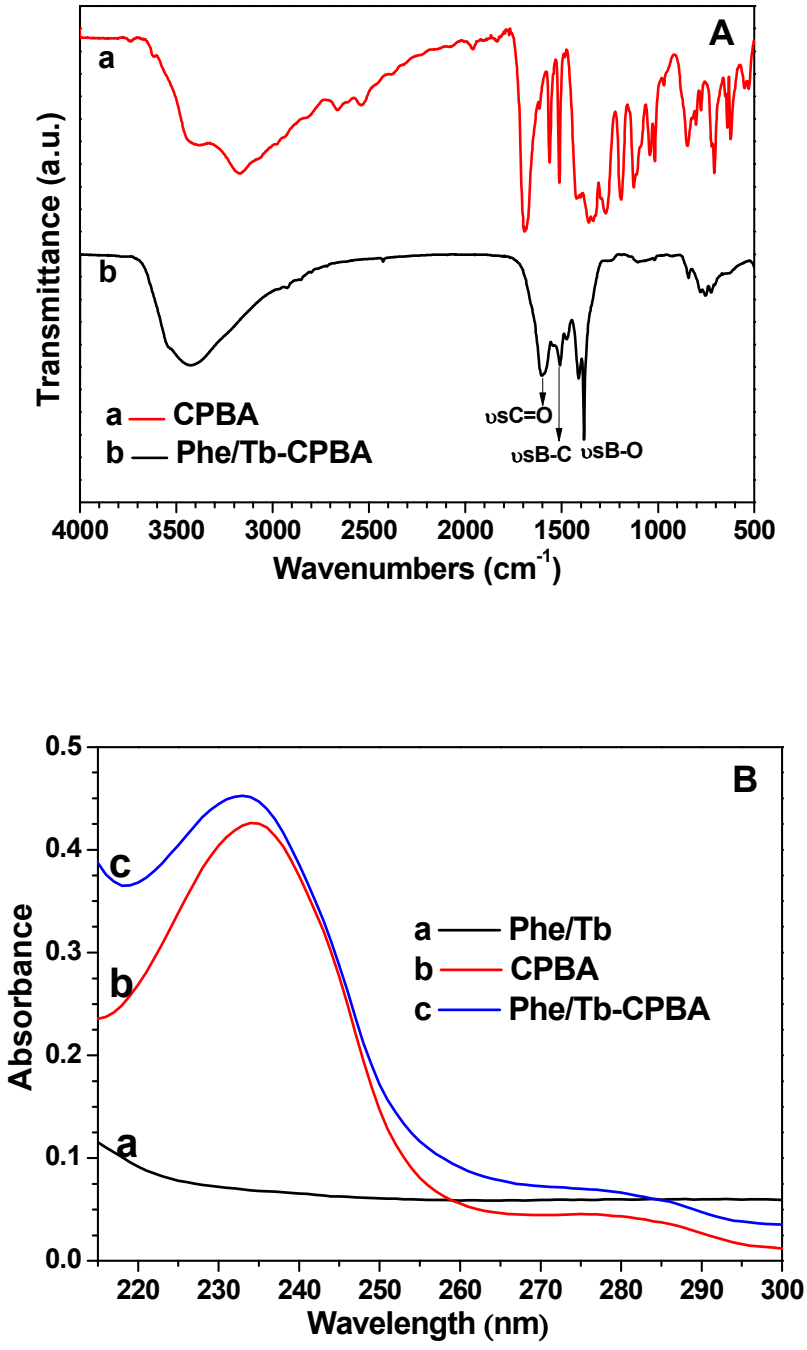

Figure 3

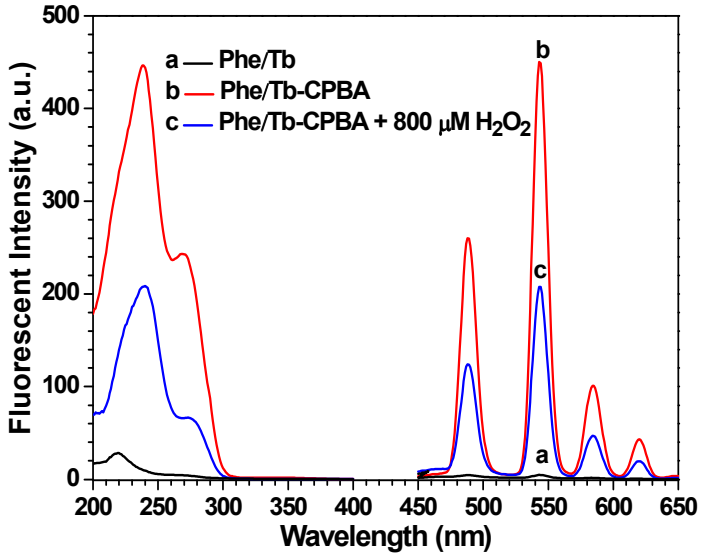

Figure 4

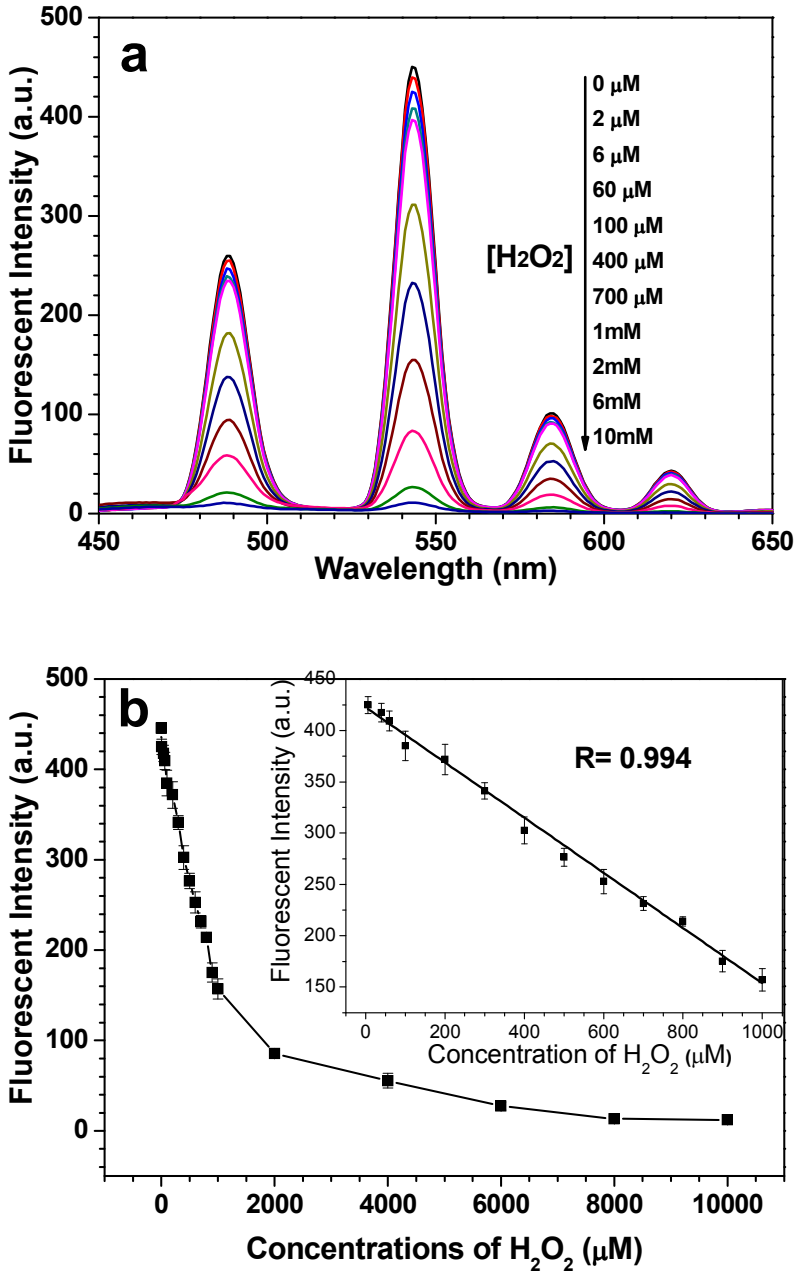

Figure 5